Published in final edited form as:
Circulation. 2015 August 11; 132(6): 490–501. doi:10.1161/CIRCULATIONAHA.114.012316.

Hck/Fgr Kinase Deficiency Reduces Plaque Growth and Stability by Blunting Monocyte Recruitment and Intraplaque Motility

Indira Medina, PhD[1,2], **Céline Cougoule, PhD**[#3,4], **Maik Drechsler, PhD**[#5], **Beatriz Bermudez, PhD**[1,6], **Rory R. Koenen, PhD**[5], **Judith Sluimer, PhD**[1], **Ine Wolfs, PhD**[1], **Yvonne Döring, PhD**[5], **Veronica Herias, PhD**[1], **Marjon Gijbels, PhD**[1], **Ilze Bot, PhD**[2], **Saskia de Jager, PhD**[2], **Christian Weber, MD**[5], **Jack Cleutjens, PhD**[1], **Theo J.C. van Berkel, PhD**[2], **Kees-Jan Sikkink, PhD, MD**[7], **Atilla Mócsai, PhD**[8], **Isabelle Maridonneau-Parini, PhD**[3,4,**], **Oliver Soehnlein, PhD, MD**[5,9,10,**], and **Erik A.L. Biessen, PhD**[1]

[1]Experimental Vascular Pathology group, Department of Pathology, CARIM, Maastricht University Medical Center, Maastricht, the Netherlands [2]Division of Biopharmaceutics, Leiden Academic Center for Drug Research, Leiden University, Leiden, the Netherlands [3]CNRS; IPBS (Institut de Pharmacologie et de Biologie Structurale), Toulouse, France [4]Université de Toulouse, Toulouse, France [5]Institute for Prevention of Cardiovascular Prevention (IPEK), LMU Munich, Germany [6]Department of Pharmacology, School of Pharmacy, University of Seville, Sevilla, Spain [7]Department of Vascular Surgery, Orbis Hospital Sittard, The Netherlands [8]Department of Physiology; Semmelweis University, Budapest, Hungary [9]Department of Pathology, Academic Medical Center (AMC), Amsterdam, the Netherlands [10]German Centre for Cardiovascular Research (DZHK), Munich Heart Alliance, Munich, Germany

[#] These authors contributed equally to this work.

Abstract

Background—Leukocyte migration is critical for the infiltration of monocytes and accumulation of monocyte derived macrophages in inflammation. Considering that Hck and Fgr are instrumental in this process, their impact on atherosclerosis and on lesion inflammation and stability was evaluated.

Methods and Results—Hematopoietic Hck/Fgr–deficient, LDLr$^{-/-}$ chimeras, obtained by bone marrow transplantation, had smaller but, paradoxically, less stable lesions with reduced macrophage content, overt cap thinning, and necrotic core expansion as most prominent features. Despite a Ly6C^{high} skewed proinflammatory monocyte phenotype, Hck/Fgr deficiency led to disrupted adhesion of myeloid cells to and transmigration across endothelial monolayers *in-vitro* and atherosclerotic plaques *in–vivo*, as assessed by intravital microscopy, flow cytometry and histological examination of atherosclerotic arteries. Moreover, Hck/Fgr deficient macrophages showed blunted podosome formation and mesenchymal migration capacity. In consequence

Correspondence: Erik A.L. Biessen, PhD, Maastricht University Medical Center, P. Debyelaan 25, 6229 HX Maastricht, The Netherlands, Phone: 0031(0)43.38.74635, Fax: 0031(0)43.38.76613, Erik.Biessen@maastrichtuniversity.nl.
** equally contributing authors

Disclosures: None.

Europe PMC Funders Author Manuscripts

transmigrated dKO macrophages were seen to accumulate in the fibrous cap, potentially promoting its focal erosion, as observed for dKO chimeras.

Conclusions—Hematopoietic deficiency of Hck and Fgr led to attenuated atherosclerotic plaque formation by abrogating endothelial adhesion and transmigration; paradoxically it also promoted plaque instability by causing monocyte subset imbalance and subendothelial accumulation, raising a note of caution regarding src kinase targeted intervention in plaque inflammation.

Keywords

kinases; mobility; atherosclerosis; immunology; leukocyte; migration; plaque progression

Introduction

Inflammation and wound healing are determinants of disease progression and clinical outcome in atherosclerosis. They are emerging as interrelated processes with overlapping molecular mechanisms controlling monocyte infiltration and differentiation into macrophages, whose phenotype determines the stability of lesions, by controlling the balance between matrix degradation and inflammation versus matrix deposition and resolution of inflammation and wound healing[1].

Monocyte/macrophage intravasation is an essential step for metabolic disease pathogenesis including atherosclerosis. The ability of monocytes to roll and adhere to the endothelium in response to chemokines is crucial for macrophage accumulation.[2] It relies on actin dependent morphological polarization, formation of filopodia and lamellipodia, binding of integrins to endothelial adhesion molecules, cytoskeletal reorganization[3] and signal transduction pathways ultimately leading to concerted loosening of adherent junctions on endothelial cells[4] and monocyte transmigration across endothelial, basement membrane and fibrous cap barriers, before their homing in expanding lesions and differentiation into pro- or anti-fibrotic macrophages.

Hck and Fgr are two Src tyrosine kinases that display restricted co-expression in myeloid cells where they regulate β2 integrin binding to endothelial ICAM to facilitate cell adhesion and migration upon PSGL-1 and CD44 interaction with endothelial E-selectin and P-selectin[5,6] In addition, Hck and Fgr are a convergence point of signaling pathways initiated by a wide range of cell receptors implicated in the pathogenesis of atherosclerosis, including integrins, immune and growth factors, Fcγ and chemokine receptors. These kinases exert their functions by activation of several effectors including Rac/CDC42, Syk and Pyk[7] which are implicated in the accumulation and trapping of macrophages in atherosclerosis.[8-11] As expected from signaling molecules targeted by multiple receptors, Hck and/or Fgr mediate a broad spectrum of processes, ranging from cell proliferation, survival and differentiation; to cytokine secretion, cytoskeleton dynamics, integrin dependent cell adhesion to the endothelium and migration.[7, 12-15]

In light of these data, we hypothesized that Hck/Fgr-deficiency would lead to reduced accumulation of macrophages in atherosclerosis onset and progression, a consequence of reduced diapedesis and migration. Our data imply that Hck and Fgr not only are

Europe PMC Funders Author Manuscripts

progressively overexpressed in atherosclerosis, but also control critical molecular processes in monocyte influx, blood monocyte subset balance, macrophage accumulation and maintenance atherosclerotic lesion stability.

Materials and Methods

Animal Experiments

Bone marrow transplantation, perivascular collar placement and intravital microscopy experiments were approved by the local regulatory authorities of Leiden and Maastricht, and performed in accordance with Dutch, French and German Government guidelines as described in the Supplemental Methods.

Cholesterol and Triglyceride Levels

Blood samples were taken by tail bleeding one day before and five weeks after introduction of Western type diet (WTD) and at sacrifice. Total plasma cholesterol, triglyceride and phospholipid contents were measured by an enzymatic-colorimetric assay (Roche Diagnostics, Almere, The Netherlands).

Plasma cytokine levels

The Luminex 100 Bio-Plex cytokine assay (Bio-Rad Laboratories, Inc; Hercules CA, USA) was used to determine plasma levels of: IL-1α, IL-1β, IL-2, IL-4, IL-5, IL-6, IL-10, IL12(P40), IL-12(P70), IL-17, Eotaxin, Keratinocyte Chemoattractant (KC), Monocyte Chemoattractant Protein-1 (MCP-1), Monocyte Inflammatory Protein-1α (MIP-1α) and Tumor Necrosis Factor-α (TNF-α). Statistical analysis was performed for the cytokines that reached the limit of detection (IL-1β, IL-12, eotaxin, MCP1 and IL–1α).

Blood Cell Analysis and Flow Cytometry

Blood, bone marrow and peritoneal cells were harvested at sacrifice and single cell suspensions prepared. Lysis of erythrocytes was performed in ice cold NH_4Cl (8.4g/l) $NaHCO_3$ (1g/l) EDTA (37mg/l) during 3 minutes. Single cell suspensions were stained with fluorescent label conjugated antibodies for different markers, and analysed by FACS as detailed in the Supplemental Methods. Whole blood samples were analyzed on a Sysmex blood cell analyzer (XT-2000i, Sysmex Europe GmbH, Norderstedt, Germany).

Cell culture

Bone marrow derived and peritoneal macrophages (BMDM and PEM), vascular smooth muscle cells (vSMC), human aortic endothelial cells (HAoEC) and Jurkat lymphocytes were cultured as detailed in the Supplemental Methods.

Thioglycolate Induced Peritonitis

Cells were collected for analysis by FACS and microscopic quantification by Giemsa staining 1, 3 or 5 days (as indicated) after induction of peritonitis with a sterile solution of dehydrated Brewer’s complete Thioglycolate (TG) broth (1ml, 2-3% w/v, Difco Laboratories, West Molesy, UK).

Phagocytosis, Apoptosis and Proliferation Assays

Proliferation and apoptosis assays, phagocytosis of apoptotic cells and zymosan particles and cholesterol uptake experiments are detailed in the Supplemental Methods.

Macrophage adhesion and transmigration across the endothelium

Endothelial HAoEC cells (PromoCell) were grown and preincubated with TNF-α (10 ng/ml) for at least 4h. Hck and Fgr mutant bone marrow derived macrophages (BMDM) or wild type (WT) controls were suspended at 5×10^5 cells/ml in 1x Hank's buffer, 20mM HEPES, 0.5% HSA (Baxter) and 1mM calcium and magnesium after stimulation with IFN-γ (100U/ml Peprotech) during 16 hours. For assessment of cell adhesion, macrophages were perfused over inflamed HAoEC monolayers during 2min at 0.1 ml/min and cells counted in 6 High Power Field (HPF, 100X magnification) pictures. Transmigration was recorded at a flow rate of 0.05ml/min for 30min in 15 sec intervals using a differential interference contrast (DIC) microscope.

Macrophage morphology, migration, podosome rosette formation and matrix degradation

Assessment of macrophage morphology, and two and three dimensional migration is detailed in the Supplemental Methods.

Gelatin zymography and β-hexosaminidase release

Zymography experiments were performed as previously described.[13] Briefly, BMDM (1×10^6 cells/well) were seeded overnight into 6-well fibronectin coated plates. Conditioned cell culture medium and cell lysate were subjected to 10% (w/v) SDS, 0.1mg/ml gelatin gel electrophoresis. For β-hexosaminidase release, BMDM were seeded overnight into 6-well plates, the assay was performed on cell extracts obtained in 1% Triton X100 and supernatants as previously described.[15]

Classical and Alternative Macrophage Polarization

BMDM (5×10^5 cells/well) were seeded in 24-well plates and allowed to adhere overnight before immune polarization was induced by 24h incubation with 100U/ml IFN-γ (Peprotech) or 20ng/ml IL-4 (Peprotech). RNA isolation, cDNA synthesis and Real Time PCR were performed as detailed in the Supplemental Methods.

SMC Collagen Synthesis and Proliferation

Cell proliferation, collagen and non-collagenous protein extracellular deposition were assessed in vascular smooth muscle (vSMC) layers by ELISA (Roche, BrdU colorimetric kit) and a quantitative collagen and protein micro-assay kit (Chondrex, Inc. Redmond, WA, USA), respectively, according to manufacturer's instructions.

Tissue Harvesting, Immunohistochemistry and Plaque Morphometry

Mice were anesthetized, sacrificed and perfused, before collection of hearts, aortas, common carotid arteries, peritoneal ascites and other organs as described in the Supplemental Material and Methods, which also contains a detailed description of cell and tissue staining and visualization procedures.

Europe PMC Funders Author Manuscripts

Analysis of microarray data

For micro-array analysis, total RNA was extracted using the Guanidine Thiocyanate (GTC)/CsCl gradient method[17] and a NucleoSpin RNA II kit (Macherey Nagel, Duren, Germany), from early (n=13) and advanced stable (n=16) lesions obtained after autopsy (Department of Pathology, University Hospital Maastricht, Maastricht, the Netherlands) or advanced stable (n=21) and advanced unstable (n=23) lesions obtained upon surgery (Department of Surgery, Maasland Hospital Sittard, Sittard, the Netherlands). RNA concentration and quality and lesion phenotype was determined as detailed in the Supplemental Methods. All human work was approved by the Ethics Committee of the University Hospital Maastricht. Written informed consent for participation in the study was obtained from all individuals. Samples from autopsy were individually hybridized to HGU133 2.0 Plus arrays (Affymetrix, Santa Clara, USA, California) and samples from surgery to Illumina Human Sentrix-8 V2.0 BeadChip® (Illumina Inc., San Diego, USA, California).

Microarray expression data of macrophage immune polarization was obtained at the Gene Expression Omnibus Web site (www.ncbi.nlm.nih.gov/geo) under accession numbers GSE18686.[18] Data normalization and summarization along with statistical, cluster and GO analysis are described in the Supplemental Methods.

Statistical Analysis of Experimental Data

Analysis were done using MatLab's Statistics ToolBox (Ver7.9) or INSTAT (Graphpad Software, Inc). Two-group comparisons were analyzed by Welch Student's t-test to account for unequal variances (except for higher powered data sets (n>8) with equivalent variance, where we opted for an unpaired t-test) Two sided P-values less than 0.05 were considered significant and denoted with one, two or three asterisks when lower than 0.05, 0.01 or 0.001, respectively. Comparisons that did not reach significance were not highlighted by an asterisk.

Figure data are presented as mean ± SEM (unless otherwise stated), while data in the result section are given as relative change compared to the WT control. Regression lines were compared by analysis of covariance (ANCOVA), using the independent variable "plaque area" as covariate and macrophage content or necrotic core size as outcome in a two-group analysis of covariance. Linear regression slopes were plotted with 95% confidence intervals. Multiple comparison analyses were analyzed by one-way ANOVA with Bonferroni correction, at a significance threshold of 0.05.

Results

Hematopoietic deficiency in Hck and Fgr reduces atherogenesis

A first indication of the participation of the src kinases HCK and FGR in atherosclerotic lesion progression was provided by their upregulation in advanced human atherosclerotic lesions, compared to early ones, GSE28829) (Suppl. Fig. 1A), while the expression of both kinases was also significantly increased in human atherosclerotic vulnerable lesions, compared with stable ones (Suppl. Fig. 1B), linking them to lesion progression.

To establish active involvement of Hck and Fgr in atherosclerosis we generated atherosclerosis prone chimeric mice by reconstitution of lethally irradiated *LDLr*$^{-/-}$ recipient animals with *Hck*$^{-/-}$*Fgr*$^{-/-}$ double knockout (dKO) or wild type (WT) bone marrow cells. Hck/Fgr deletion did not lead to any alteration in total body weight along the experiment nor did it affect plasma total cholesterol levels before (199.4 mg/dl vs. 150.8 mg/dl for WT controls), and after (1616.1 mg/dl vs. 1488.9 mg/dl, for WT controls) western type diet (WTD) introduction. Plasma levels of proinflammatory cytokines such as IL–1β, IL–12, eotaxin, MCP1, and IL–1α, as measured at sacrifice, were not influenced by Hck/Fgr-deficiency (Suppl. Fig. 1C).

Western type diet fed chimeric mice transplanted with Hck/Fgr dKO bone marrow exhibited 30% (P≤0.05) reduction in intermediate atherosclerotic lesion size (Fig. 1A), while at later stages of plaque progression it led to 40% smaller plaques (P≤0.01; Fig. 1B+C).

Unexpectedly, despite their reduced size, plaques from Hck/Fgr dKO chimeras exhibited a more vulnerable plaque phenotype, characterized by necrotic core expansion, (+68%; P≤0.01; Fig 1D) and significant reductions in collagen and SMC (−75% and −82%, respectively, both P≤0.001; Fig.1 E-F) and fibrous cap thickness (−53%, P≤0.001) (Fig. 1G +H). The apoptotic rate in early lesions, as measured by caspase-3 staining, did not differ between dKO versus WT chimeras (Fig. 1I). The diminished plaque fibrosis was coupled with 34% (P≤0.001; Fig.1J-K) and 61% (P≤0.05; Fig.1L-M) reductions in intimal macrophage and adventitial neutrophil contents, respectively. As plaque cell proliferation, assessed by Ki67 staining, was unchanged (Fig 1N), it is unlikely that the reduced plaque macrophage content results from HCK/FGR deficiency associated effects on plaque macrophage expansion. Statistical regression analysis revealed that although necrotic core size and plaque macrophage content were both associated with plaque size (P≤0.001 for both), neither of the two did so in a genotype-dependent manner, indicating that the changes in plaque macrophage content and necrotic core size reflected a delayed plaque progression (Suppl. Fig. 1D+E). The reduced presence of (F4/80^{+}) plaque macrophages in dKO vs WT chimeras was confirmed by flow cytometry analysis of aorta (−42%, P≤0.001), whereas vascular CD3^{+}-T lymphocyte content was unchanged (Fig.2A-B). This aligns well with the observation that Hck and Fgr showed highest expression in myeloid cells at mRNA (Fig.2C) as well as protein level (Fig.2D). To address whether the diminution of plaque macrophage and neutrophil numbers was caused by a reduced availability of myeloid subsets in dKO chimeras, we studied the impact of Hck/Fgr deficiency on myeloid versus non myeloid subset patterns in blood, spleen and bone marrow. The absolute and relative levels of circulatory, bone marrow and spleen white blood cells, T (cytotoxic, helper and Tregs) and B lymphocytes, as well as spleen dendritic cells (DCs, resident and plasmacytoid), were not disturbed in WTD fed dKO chimeric mice (data not shown). compared to WT controls. Similarly, equivalent myeloid cell composition (Suppl. Fig. 2A) and monocyte subset levels (Suppl. Fig. 2B) were observed in bone marrow. Expression of Ly6C was not influenced by lack of Hck/Fgr in Ly6C^{low} and Ly6C^{high} blood monocytes subsets. This suggests that the increased Ly6C is not owing to deficiency of Fgr, which was seen to bind Ly6C and activate LFA-1 [19] (Suppl. Fig. 2C-E). Similarly, absolute or relative levels of circulatory granulocytes and monocytes were unchanged (Suppl. Fig. 2F-I). Relative Ly6C^{high}

monocyte abundance (+47%, P≤0.01) was however significantly increased (Suppl. Fig. 2J), which generally is thought to be associated with increased invasion into atherosclerotic lesions. Nevertheless, significantly less leukocytes (Fig. 2E) and in particular less monocytes/macrophages (Fig. 2F-G) were recruited to the peritoneal cavity of dKO chimeras in a model of thioglycolate (TG) induced peritonitis. The expression of monocyte chemotaxis mediating chemokine receptors (CCR2, CCR5, CXCR1-3 and CX_3CR1) by sorted $Ly6C^{high}$ bone marrow monocytes was unchanged (Suppl. Fig. 1F); likewise DKO macrophages did not display altered expression of chemokines CCL2 and CCL5 (Suppl. Fig. 1G). This suggests that the reduced macrophage invasion into inflamed peritoneum or plaque is not owing to aberrant chemotaxis. No differences in the activation of macrophages were observed, as assessed by the expression of CD86, CD40 and MHCII (Fig. 2H); indicating that Hck/Fgr-deficiency did not perturb the activation potential of macrophages, a result which could be relevant for atherosclerotic lesion macrophages.

Lack of Hck/Fgr leads to reduced leukocyte adhesion to the endothelium

Echoing the reduced accumulation of dKO macrophages in peritonitis and atherosclerotic lesions, we found that adoptively transferred fluorescently labeled dKO bone marrow derived macrophages (BMDM) displayed profoundly reduced adhesion (−67%, P≤0.001) and almost ablated transmigration (−88%; P≤0.001) to preexisting collar induced carotid artery lesions induced in western type diet fed *LDLr*$^{-/-}$ mice (Fig. 3A-C). Next we performed intravital microscopy analysis at the carotid artery bifurcation of WTD fed WT vs dKO chimeras after *in situ* labeling of circulating leukocytes (Rhodamine G or Rho), $CD11b^+$ monocytes, $CD11b^+$ $Ly6C^{high}$ monocytes and $Ly6G^+$ neutrophils. Concordant with the aforementioned adoptive transfer studies plaque neutrophil and monocyte adhesion, were sharply reduced (P≤0.001 for all) (Fig.3 D-E), at which the effects on $CD11b^+$ $Ly6C^{high}$ monocytes seemed to be most pronounced. Extending this finding we sought to track the dynamics and more in particular the plaque homing capacity of pro-inflammatory $LyC6^{hi}$ monocytes in WT versus Hck/Fgr deficient mice. Hereto we employed the $Ly6C^{high}$ monocyte specific latex labeling procedure described by Tacke et al[20] and observed reduced amounts of Latex bead-laden $Ly6C^{high}$ cell derived macrophages in plaque 24h after bead labeling as witness flow cytometry and fluorescent microscopy analysis (Fig 3.F-H).

To be able to dissect the individual steps in monocyte recruitment to the plaque, we performed flow experiments. DKO BMDM perfused through a monolayer of inflamed endothelium *in vitro* displayed reduced adhesion (−52%; P<0.05; Fig. 4A-B). However, the percentage of adherent cells able to transmigrate across the endothelium *in vitro* was not influenced by Hck/Fgr-deficiency (Fig. 4C), implying that the inhibited trans-endothelial macrophage migration mainly reflects the prior impairment of the adhesion mechanism. This intriguing observation led us to investigate the (trans)migration process in closer detail. *In vitro*, dKO BMDM displayed almost ablated wound invasion in a wound healing assay (−94%, P≤0.001; Fig. 4D), despite that proliferation rates under baseline and LPS stimulated conditions (Suppl. Fig. 3A) and seeded cell densities were similar in both genotypes, indicating impaired two-dimensional migration. In addition, dKO peritoneal macrophages (PEM) presented altered morphology *in vitro*, characterized by lack of elongation (−56%, P≤0.001) and morphological polarization (P≤0.001), while the cells were also featuring

sharply reduced filopodium and lamellopodium formation (Fig. 4E-I); suggestive of dysfunctional actin network polymerization.

Taken together these results indicate impaired adhesion and two-dimensional crawling on the endothelium previous to diapedesis, as contributing factors to the reduced macrophage accumulation observed in atherosclerotic dKO chimeras.

Hck/Fgr-deficient macrophages display reduced three-dimensional migration

We next assessed the three-dimensional migration capacity of dKO macrophages, taking into account that particularly at later stages of lesion progression, extravasated cells must pass through collagen and smooth muscle cell (SMC) rich fibrous caps. Macrophages employ mesenchymal and amoeboid migration mechanisms to perform three-dimensional infiltration[21] either by protease-dependent degradation of dense extracellular matrices (ECM) or by squeezing and deforming their cell body into ECM pores, respectively. *In vitro*, dKO BMDM displayed unimpeded amoeboid migration across type I fibrillar collagen (Fig 5A), which contrasted with their markedly inhibited mesenchymal migration through dense Matrigel (Fig 5B). Furthermore, the addition a cocktail of protease inhibitors (PI) inhibited the mesenchymal migration through Matrigel in WT BMDM to levels observed in untreated mutant cells. It however failed to impact the migration capacity of mutant BMDM (Fig. 5B). This suggests that Hck/Fgr deficiency associated ablation of mesenchymal migration implicates protease activity. Next, we examined whether dKO BMDM display abnormal secretion of proteases. The release of the lysosomal hydrolase β-hexosaminidase (Fig. 5C), as well as of MMP2 and MMP9 was however not affected (Fig. 5D), excluding vesicular secretion defects to have underlain the observed impairment of macrophage migration.[21] The mesenchymal migration of macrophages requires cell adhesion and extracellular matrix degrading structures called podosomes.[22-24] As we already have shown, macrophage podosome stability and function are regulated by Hck in macrophages.[13,16] BMDM from WT mice formed large podosome rosettes; dKO cells, in contrast, formed fewer and smaller podosome rosettes (Fig. 5E-F). As a consequence, focal ECM degradation capacity of dKO macrophages as assessed by FITC gelatin degradation, was significantly decreased as compared to their WT counterpart (Fig. 5G-H).

Taken together these results indicate that Hck/Fgr gene deletion causes reduced mesenchymal migration by impairing the formation of podosome rosettes leading to diminished pericellular degradation of the extracellular matrix. This potentially has major implications for the invasive capacity of extravasated plaque macrophages. Therefore we have histologically re-inspected the plaque for presence and location of latex bead-labeled cells in the monocytes/macrophages tracking study described in figure 3. In keeping with the impaired mesenchymal migration capacity *in vitro*, we observed that significantly less latex$^+$ macrophages had migrated beyond the basal membrane into the plaque atheroma (−58%, $P<0.001$; Fig.5I). Moreover, the average invasion depth of latex$^+$ positive macrophages that had invaded into the plaque at 24h after labeling was sharply reduced as well (−77%; $P\leq0.01$; Fig 5J).

Hck/Fgr-deficient macrophages display impaired efferocytosis and an anti-fibrotic phenotype

The subendothelial accumulation of macrophages could have contributed to the more vulnerable phenotype of dKO chimeras versus their WT counterparts, as hallmarked by reduced fibrosis and cap thinning. As features of plaque vulnerability are often associated with disbalanced extracellular matrix homeostasis, owing to the pro-inflammatory; collagen synthesis inhibitory, and erosive milieu presented by plaque macrophages, in particular if polarized towards a classically activated phenotype.[1] Moreover Ly6C^{high} monocytosis, as observed in dKO chimeras (Suppl. Fig. 2J), by itself has already been linked to preferential polarization towards classically activated macrophages (CAM).[25]

Therefore we investigated if Hck/Fgr-deficiency has impacted macrophage phenotype. We first assessed whether macrophage polarization itself influences Hck/Fgr expression by transcriptome analysis of differentially expressed genes from human macrophages stimulated with TNF-α, IL-4, IL-17 LPS, IFN-γ or LPS+IFN-γ (GSE18686[18]). Hck and Fgr are included in separate gene networks, as revealed by K-means cluster analysis (C-IV and C-III, respectively) (Fig.6A). Principal component analysis indicated that C-III and C-IV contained genes with upregulated expression in response to alternative (IL-4) and classic (LPS, IFN-γ or LPS+IFN-γ) stimulants, respectively (Fig. 6B). Consistently, Hck and Fgr were more than two fold upregulated in response to IFN-γ and IL-4 respectively (Fig. 6C), suggesting their divergent participation in classic and alternatively activated macrophage (AAM) molecular networks, respectively. This was confirmed at the protein level by western blotting on naïve and primed BMDM from WT and dKO mice, showing a tendency towards increased Hck expression by classically activated macrophages (CAM) and increased Fgr by AAM (Fig. 6D-E). Although conclusive evidence is lacking, CAM are believed to represent the dominant phenotype in plaque. This therefore implies a major role for Hck in plaque macrophage function, as also suggested by the upregulation of Hck in advanced rupture-prone human atherosclerotic lesions (Suppl. Fig. 1A+B)

However, analysis of polarization marker gene expression failed to demonstrate consistent Hck/Fgr deficiency associated changes in macrophage phenotype. Baseline mRNA expression of established classically activated macrophage markers by non-stimulated BMDM such as iNOS, IL-12 or TNFα was essentially unchanged, as was that of the alternatively activated macrophage markers arginase-1 and the mannose receptor (Fig 6F). Likewise, polarization marker gene expression by LPS+IFN-γ or IL-4 primed WT and dKO BMDM were largely similar (Suppl Fig. 3B and C, resp). At the protein level, dKO and WT BMDM showed equivalent IL-12 secretion, while TNFα production was slightly increased (Suppl Fig. 3D) and that of NO was significantly reduced (Suppl Fig. 3E). Concordant with these data, mRNA expression analysis on isolated aorta did not reveal major changes in macrophage polarization marker expression pattern, apart from a slight increase in CD206 expression (Fig. 6G), while iNOS^{+} and arg-1^{+} macrophage content in intermediate lesions did not point to a shift towards classical macrophage activation in dKO vs WT chimeras either (Fig. 6H-I).

Europe PMC Funders Author Manuscripts

As the complexity of macrophage adaptive responses in vivo cannot be completely captured by the rigid dichotomy of the macrophage polarization model *in vitro* we zoomed in on Src kinase associated differences in macrophage functions, that could underlie dKO associated plaque destabilization. First we assessed whether Hck/Fgr deficiency impacts macrophage cell death or their ability to ingest particles, opsonized particles, and cholesterol accumulation, functions which are potentially controlled by src kinases and are relevant to plaque stability. Hck/Fgr-deficient BMDM exposed normal apoptotic susceptibility (Suppl. Fig. 4A), phagocytosis of fluorescent Latex beads or opsonized particles (Suppl. Fig. 4B-C), and uptake of modified cholesterol, *in vitro*, as assessed by HPTLC or fluorescent microscopy (Suppl. Fig. 4D-E). Efferocytosis, defined as the macrophage capacity to process apoptotic cells, was however considerably reduced in dKO BMDM (Suppl. Fig. 4F), which could at least partially explain the necrotic core expansion observed in dKO chimeras.

Interestingly, incubation of vascular smooth muscle cells with conditioned medium from non-stimulated dKO BMDM did not influence their proliferation (Suppl. Fig. 5A), but reduced their deposition of extracellular collagen and non-collagenous proteins akin to conditioned medium from LPS-primed WT macrophages and starvation medium (Suppl. Fig. 5B-C). Apparently, Hck/Fgr-deficiency favors a macrophage anti-fibrotic differentiation phenotype, and we propose that the impact of this effect will even be amplified by the reduced mesenchymal migration into the plaque of dKO macrophages, conducing to increased focal accumulation of antifibrotic macrophages in close proximity to the fibrous cap.

Discussion

Here we present conclusive evidence that Hck/Fgr-deficiency leads to reduced atherosclerotic lesion burden with concomitant reductions in macrophage accumulation and, paradoxically, lesion stability. As we show the former is due to impaired adhesion of macrophages to the endothelium, while the latter is likely attributable to blunted mesenchymal migration into the plaque atheroma, resulting in the retention of lytic macrophages in the plaque's fibrous cap. As a first hallmark of Hck/Fgr-deficiency, atherosclerotic lesions displayed reduced amounts of macrophages despite the marked skewing of monocyte differentiation towards a Ly6C^{high} phenotype, a subset known for its hypermigratory and proinflammatory profile, and selective accumulation in atherosclerosis.[20,25]

With use of intra- and extravital microscopy analysis of fluorescent dye, antibody and latex bead labeled leukocyte subsets, we were able to firmly establish Hck/Fgr deficiency-induced impairment of monocyte and neutrophil adhesion to and diapedesis into plaque, while their chemotactic profile remained unaffected. This finding was confirmed by post-hoc immunohistochemical analysis of plaque for the presence of latex bead-laden macrophages. The reduced presence of (Ly6C^{hi}) monocyte derived macrophages is especially remarkable given the relative abundance of circulating Ly6C^{high} monocytes in dKO chimeras. This subset is thought to be associated with higher Ly6C^{high} monocyte infiltration[20,25] and reduced accumulation of pro-fibrotic and anti-inflammatory macrophages.[26] It should be noted however that the Ly6C^{low} subset has been shown to contribute to plaque inflammation

at later stages of disease development and has repeatedly been linked to plaque vulnerability and fibrosis.[27-29]

In addition, Hck/Fgr-deficient macrophages featured an impaired morphological polarization, and disrupted two-dimensional migration. DKO macrophages were unable to form filopodia and lamellipodia, which is critical for those cells to adhere and establish leading and trailing poles that direct their mobilization towards higher concentrations of chemoattractants.[30] Taken together, these results imply that Hck/Fgr-deficiency results in reduced adhesion and directional crawling on the endothelium and therefore in impaired extravasation of circulating monocytes into the atherosclerotic lesion. The three-dimensional mesenchymal migration of macrophages depends on the formation of podosome rosettes, which release proteolytic enzymes to perform pericellular degradation of the extracellular matrix.[21] *In vitro*, dKO macrophages exhibited an attenuated focal degradation of extracellular matrix, disrupted formation of podosome rosettes, and accordingly disrupted mesenchymal migration. Extrapolating these findings to atherosclerosis, Hck/Fgr-deficiency has impacted both the adhesion of monocytes to the plaque as well their mesenchymal migration across the lesional fibrous cap, contributing to the striking reduction in plaque macrophage content and to subendothelial accumulation of invaded macrophages.

A second striking hallmark of Hck/Fgr-deficiency in atherosclerosis was the paradoxical induction of necrotic core expansion and lesion vulnerability, with reduced fibrosis, SMC accumulation and collagen deposition. This phenotype is remarkably similar to that observed in ear excision wounds treated with Src tyrosine kinase inhibitors,[31] alluding to a positive role of Hck/Fgr in macrophage pro-fibrotic functions. Compatible with the latter, conditioned medium from dKO macrophages was seen to reduce collagen production by vascular smooth muscle cells. The impact of this plaque destabilizing effect will be considerably augmented by the increased retention of extravasated, migration-defective dKO monocytes in subendothelial tissue close to the fibrous cap, where they can exert their cap erosive functions.

Our experiments thus underpin the importance of Hck/Fgr not only in migration but also in macrophage pro-fibrotic differentiation. Analysis of microarray datasets and our gene expression studies point to divergent regulation of Hck and Fgr expression in response to macrophage classical and alternative polarization, supportive of a role for these kinases in the spectrum of macrophage immune differentiation. However, we did not observe consistent Hck/Fgr deficiency associated shifts in macrophage polarization marker expression. But, Hck/Fgr-deficient macrophage displayed functional changes relevant to plaque stability, with inhibited SMC extracellular matrix protein deposition, and reduced efferocytosis capacity as most prominent features.

In conclusion, Hck and Fgr deficiency is associated with a reduced recruitment of myeloid cells to the plaque, despite the observed skewing of monocytes towards the pro-inflammatory Ly-6C^{hi} monocytes. However, the beneficial effects of reduced leukocyte influx is counteracted by the focal retention of extravasated monocytes in the fibrous cap, promoting its erosion and plaque vulnerability. The apparent pro-fibrotic function of Hck/Fgr raises a note of caution against the use of Src kinase inhibitors for the treatment of

atherosclerosis, where reduced macrophage accumulation and fibrous cap integrity are desired to attain a stable plaque profile. However, their novel application as anti-fibrotic therapy in systemic sclerosis[32,33] and our results, support their potential to treat fibroblastic vasculopathies such as restenosis and disorders where simultaneous reduction of fibrosis and macrophage accumulation are desired.

Supplementary Material

Refer to Web version on PubMed Central for supplementary material.

Acknowledgements

We thank M Waqar Aslam for technical assistance with opsonized particle phagocytosis assays and TRI (Toulouse Réseau Imagerie) and Anexplo GenoToul facilities at the IPBS (Toulouse). We also thank Dr Lowell CA (University of California, San Francisco, USA) who kindly provided the Hck/Fgr deficient mice.

Funding Sources: This work was supported in part by the Netherlands Organization for Scientific Research (# 912.02.037, IM; grant 916.86.046, IB; grant 91712303, OS), by the Netherlands Heart Foundation (grant D2003T201, EB, SdJ), by the European Community's Seventh Framework Program under grant agreement HEALTH-F4-2011-282095 (CC, IMP), by the Agence Nationale de la Recherché,(grant 2010-01301; CC, IMP), by the Fondation pour la Recherche Médicale (DEQ 20110421312;CC, IMP), by the European Union (TARKINAID project; Grant No. 282095 (AM), and by the DFG (SO876/6-1, SFB914 TP B08, SFB1123 TP A6 and B5). EB is Established Investigator of the Netherlands Heart Foundation (D2003T201); AM is a Senior Research Fellow of the Wellcome Trust (Grant No. 087782).

References

1. Murray PJ, Wynn TA. Protective and pathogenic functions of macrophage subsets. Nat Rev Immunol. 2011; 11:723–737. [PubMed: 21997792]
2. Ley K, Laudanna C, Cybulsky MI, Nourshargh S. Getting to the site of inflammation: the leukocyte adhesion cascade updated. Nat Rev Immunol. 2007; 7:678–689. [PubMed: 17717539]
3. Rikitake Y, Takai Y. Directional cell migration regulation by small G proteins, nectin-like molecule-5, and afadin. Int Rev Cell Mol Biol. 2011; 287:97–143. [PubMed: 21414587]
4. Muller WA. Mechanisms of leukocyte transendothelial migration. Annu Rev Pathol. 2011; 6:323–344. [PubMed: 21073340]
5. Yago T, Shao B, Miner JJ, Yao L, Klopocki AG, Maeda K, Coggeshall KM, McEver RP. E-selectin engages PSGL-1 and CD44 through a common signaling pathway to induce integrin alphaLbeta2-mediated slow leukocyte rolling. Blood. 2010; 116:485–494. [PubMed: 20299514]
6. Zarbock A, Abram CL, Hundt M, Altman A, Lowell CA, Ley K. PSGL-1 engagement by E-selectin signals through Src kinase Fgr and ITAM adapters DAP12 and FcR gamma to induce slow leukocyte rolling. J Exp Med. 2008; 205:2339–47. [PubMed: 18794338]
7. Baruzzi A, Caveggion E, Berton G. Regulation of phagocyte migration and recruitment by Src-family kinases. Cell Mol Life Sci. 2008; 65:2175–2190. [PubMed: 18385944]
8. Harb D, Bujold K, Febbraio M, Sirois MG, Ong H, Marleau S. The role of the scavenger receptor CD36 in regulating mononuclear phagocyte trafficking to atherosclerotic lesions and vascular inflammation. Cardiovasc Res. 2009; 83:42–51. [PubMed: 19264766]
9. Hilgendorf I, Eisele S, Remer I, Schmitz J, Zeschky K, Colberg C, Stachon P, Wolf D, Willecke F, Buchner M, Zirlik K, Ortiz-Rodriguez A, Lozhkin A, Hoppe N, von zur Muhlen null C, zur Hausen null A, Bode C, Zirlik A. The oral spleen tyrosine kinase inhibitor fostamatinib attenuates inflammation and atherogenesis in low-density lipoprotein receptor-deficient mice. Arterioscler Thromb Vasc Biol. 2011; 31:1991–1999. [PubMed: 21700926]
10. Katsume A, Okigaki M, Matsui A, Che J, Adachi Y, Kishita E, Yamaguchi S, Ikeda K, Ueyama T, Matoba S, Yamada H, Matsubara H. Early inflammatory reactions in atherosclerosis are induced by proline-rich tyrosine kinase/reactive oxygen species-mediated release of tumor necrosis factor-

alpha and subsequent activation of the p21Cip1/Ets-1/p300 system. Arterioscler Thromb Vasc Biol. 2011; 31:1084–1092. [PubMed: 21372295]

11. Shah Z, Kampfrath T, Deiuliis JA, Zhong J, Pineda C, Ying Z, Xu X, Lu B, Moffatt-Bruce S, Durairaj R, Sun Q, Mihai G, Maiseyeu A, Rajagopalan S. Long-term dipeptidyl peptidase 4 inhibition reduces atherosclerosis and inflammation via effects on monocyte recruitment and chemotaxis. Circulation. 2011; 124:2338–2349. [PubMed: 22007077]
12. Berton G, Mócsai A, Lowell CA. Src and Syk kinases: key regulators of phagocytic cell activation. Trends Immunol. 2005; 26:208–214. [PubMed: 15797511]
13. Cougoule C, Le Cabec V, Poincloux R, Al Saati T, Mège J-L, Tabouret G, Lowell CA, Laviolette-Malirat N, Maridonneau-Parini I. Three-dimensional migration of macrophages requires Hck for podosome organization and extracellular matrix proteolysis. Blood. 2010; 115:1444–1452. [PubMed: 19897576]
14. Bhattacharjee A, Pal S, Feldman GM, Cathcart MK. Hck is a key regulator of gene expression in alternatively activated human monocytes. J Biol Chem. 2011; 286:36709–36723. [PubMed: 21878628]
15. Lowell CA. Src-family and Syk kinases in activating and inhibitory pathways in innate immune cells: signaling cross talk. Cold Spring Harb Perspect Biol. 2011; 3:pii, a002352.
16. Cougoule C, Carréno S, Castandet J, Labrousse A, Astarie-Dequeker C, Poincloux R, Le Cabec V, Maridonneau-Parini I. Activation of the lysosome-associated p61Hck isoform triggers the biogenesis of podosomes. Traffic. 2005; 6:682–694. [PubMed: 15998323]
17. Sambrook, J.; Russell, DW. Extraction, Purification and Analysis of mRNA from Eukaryotic cells. In: Argentine, J.; Irwin, N.; Janssen, KA.; Curtis, S.; Zierler, M., editors. Molecular Cloning: A Laboratory Manual. Cold Spring Harbor Laboratory Press; Cold Spring Harbor, New York: 2001. p. 7.4-7.9.
18. Fuentes-Duculan J, Suárez-Fariñas M, Zaba LC, Nograles KE, Pierson KC, Mitsui H, Pensabene CA, Kzhyshkowska J, Krueger JG, Lowes MA. A subpopulation of CD163- positive macrophages is classically activated in psoriasis. J Invest Dermatol. 2010; 130:2412–2422. [PubMed: 20555352]
19. Hatakeyama S, Iwabuchi K, Ogasawara K, Good RA, Onoé K. The murine c-fgr gene product associated with Ly6C and p70 integral membrane protein is expressed in cells of a monocyte/macrophage lineage. Proc Natl Acad Sci U S A. 1994; 91:3458–62. [PubMed: 8159769]
20. Tacke F, Alvarez D, Kaplan TJ, Jakubzick C, Spanbroek R, Llodra J, Garin A, Liu J, Mack M, van Rooijen N, Lira SA, Habenicht AJ, Randolph GJ. Monocyte subsets differentially employ CCR2, CCR5, and CX3CR1 to accumulate within atherosclerotic plaques. J Clin Invest. 2007; 117:185–194. [PubMed: 17200718]
21. Van Goethem E, Poincloux R, Gauffre F, Maridonneau-Parini I, Le Cabec V. Matrix architecture dictates three-dimensional migration modes of human macrophages: differential involvement of proteases and podosome-like structures. J Immunol. 2010; 184:1049–1061. [PubMed: 20018633]
22. Van Goethem E, Guiet R, Balor S, Charrière GM, Poincloux R, Labrousse A, Maridonneau-Parini I, Le Cabec V. Macrophage podosomes go 3D. Eur J Cell Biol. 2011; 90:224–236. [PubMed: 20801545]
23. Wiesner C, Le-Cabec V, El Azzouzi K, Maridonneau-Parini I, Linder S. Podosomes in space: Macrophage migration and matrix degradation in 2D and 3D settings. Cell Adh Migr. 2014; 8:179–91. 12. [PubMed: 24713854]
24. Murphy DA, Courtneidge SA. The ‘ins’ and ‘outs’ of podosomes and invadopodia: characteristics, formation and function. Nat Rev Mol Cell Biol. 2011; 12:413–426. [PubMed: 21697900]
25. Swirski FK, Libby P, Aikawa E, Alcaide P, Luscinskas FW, Weissleder R, Pittet MJ. Ly-6Chi monocytes dominate hypercholesterolemia-associated monocytosis and give rise to macrophages in atheromata. J Clin Invest. 2007; 117:195–205. [PubMed: 17200719]
26. Robbins CS, Swirski FK. The multiple roles of monocyte subsets in steady state and inflammation. Cell Mol Life Sci. 2010; 67:2685–2693. [PubMed: 20437077]
27. Combadière C, Potteaux S, Gao JL, Esposito B, Casanova S, Lee EJ, Debré P, Tedgui A, Murphy PM, Mallat Z. Decreased atherosclerotic lesion formation in CX3CR1/apolipoprotein E double knockout mice. Circulation. 2003; 107:1009–16. 25. [PubMed: 12600915]

28. Cheng C, Tempel D, van Haperen R, de Boer HC, Segers D, Huisman M, van Zonneveld AJ, Leenen PJ, van der Steen A, Serruys PW, de Crom R, Krams R. Shear stress-induced changes in atherosclerotic plaque composition are modulated by chemokines. J Clin Invest. 2007; 117:616–26. [PubMed: 17304353]

29. Martínez-Hervás S1, Vinué A, Núñez L, Andrés-Blasco I, Piqueras L, Real JT, Ascaso JF, Burks DJ, Sanz MJ, González-Navarro H. Cardiovasc Res. 2014; 103:324–36. [PubMed: 24788416] Insulin resistance aggravates atherosclerosis by reducing vascular smooth muscle cell survival and increasing CX3CL1/CX3CR1 axis.

30. Ridley AJ. Life at the leading edge. Cell. 2011; 145:1012–1022. [PubMed: 21703446]

31. Sun X, Phan TN, Jung SH, Kim SY, Cho JU, Lee H, Woo SH, Park TK, Yang B-S. LCB 03-0110, a novel pan-discoidin domain receptor/c-Src family tyrosine kinase inhibitor, suppresses scar formation by inhibiting fibroblast and macrophage activation. J Pharmacol Exp Ther. 2012; 340:510–519. [PubMed: 22128347]

32. Skhirtladze C, Distler O, Dees C, Akhmetshina A, Busch N, Venalis P, Zwerina J, Spriewald B, Pileckyte M, Schett G, Distler JHW. Src kinases in systemic sclerosis: central roles in fibroblast activation and in skin fibrosis. Arthritis Rheum. 2008; 58:1475–1484. [PubMed: 18438865]

33. Beyer C, Distler O, Distler JHW. Innovative antifibrotic therapies in systemic sclerosis. Curr Opin Rheumatol. 2012; 24:274–280. [PubMed: 22450392]

Europe PMC Funders Author Manuscripts

Europe PMC Funders Author Manuscripts

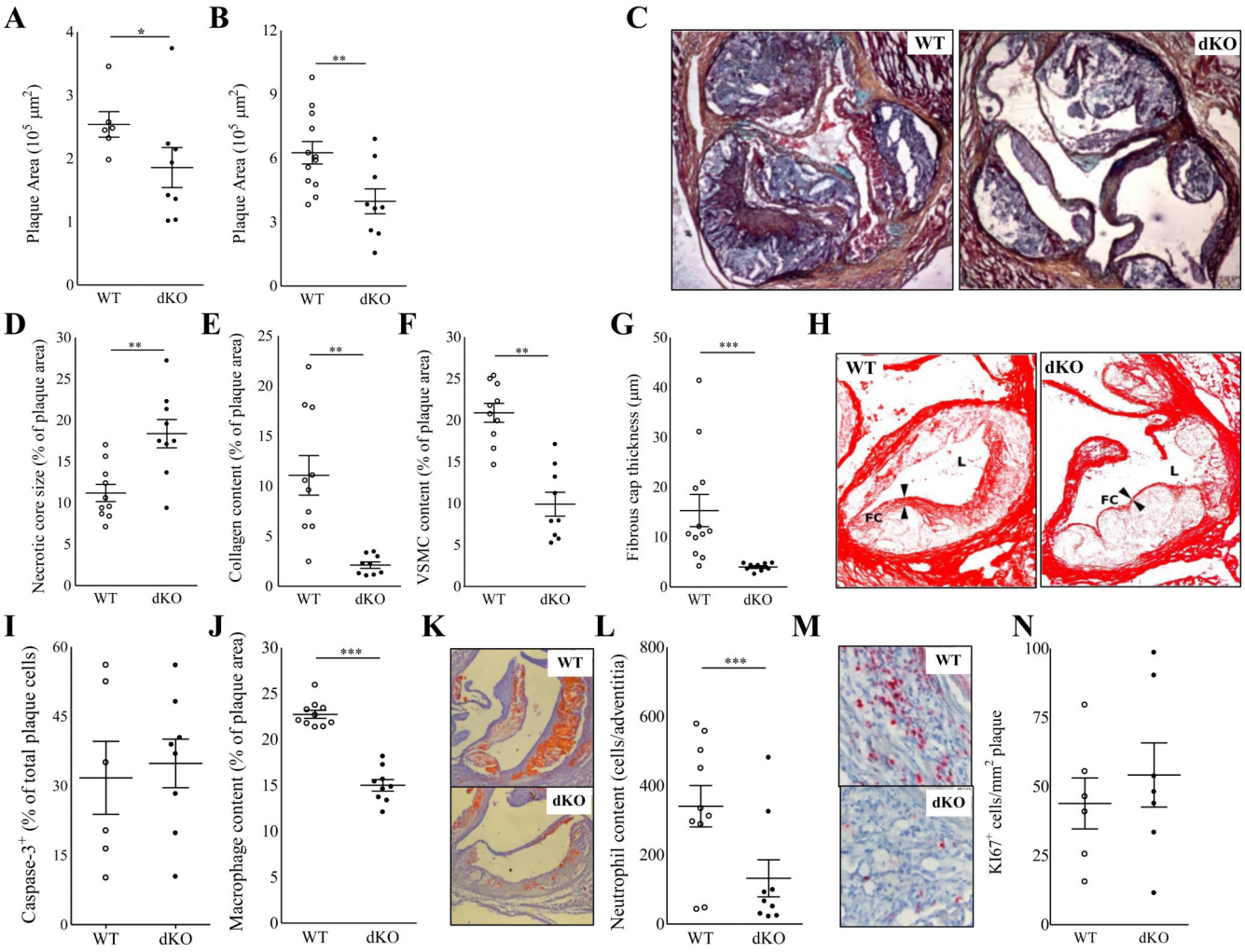

Figure 1.

A-N Reduced lesion size and altered lesion composition in Hck/Fgr dKO chimeras. Hck/Fgr-deficiency led to reduced formation of intermediate (−29%, n=8, 10 sections analyzed per unit) (A) and advanced lesions (−37%, n=13, 10 sections per unit) (B) in aortic roots of western type diet fed LDLr$^{-/-}$ mice. (C) Representative Movat stained advanced plaque sections. Advanced lesions from Hck/Fgr dKO chimeras displayed features of plaque vulnerability characterized by bigger necrotic cores (+68%) (D), reduced collagen (−82%) (E) and reduced SMC (−75%) contents (F) and thinner fibrous caps (−53%) (G) (n=13, 6 sections per experimental unit). (H) Representative pictures corresponding to D-G denoting lumen size (L) necrotic core (NC) expansion, fibrous cap (FC) thinning and diminished collagen area (Picrosirius Red staining in dKO chimeras.) (I) Lesion caspase 3^{+} cell content was unchanged in Hck/Fgr deficiency. Intimal macrophages (J+K) and adventitial neutrophils (L+M), were reduced by 34% and 61%, respectively, in advanced lesions Panels K and M display representative slides of macrophage and neutrophil stainings, respectively. Lesions of dKO mice showed similar Ki67^{+} cell content, reflecting unchanged proliferation (N). WT: open circles; dKO: filled circles; *P≤0.05, **P≤0.01, ***P≤0.001.

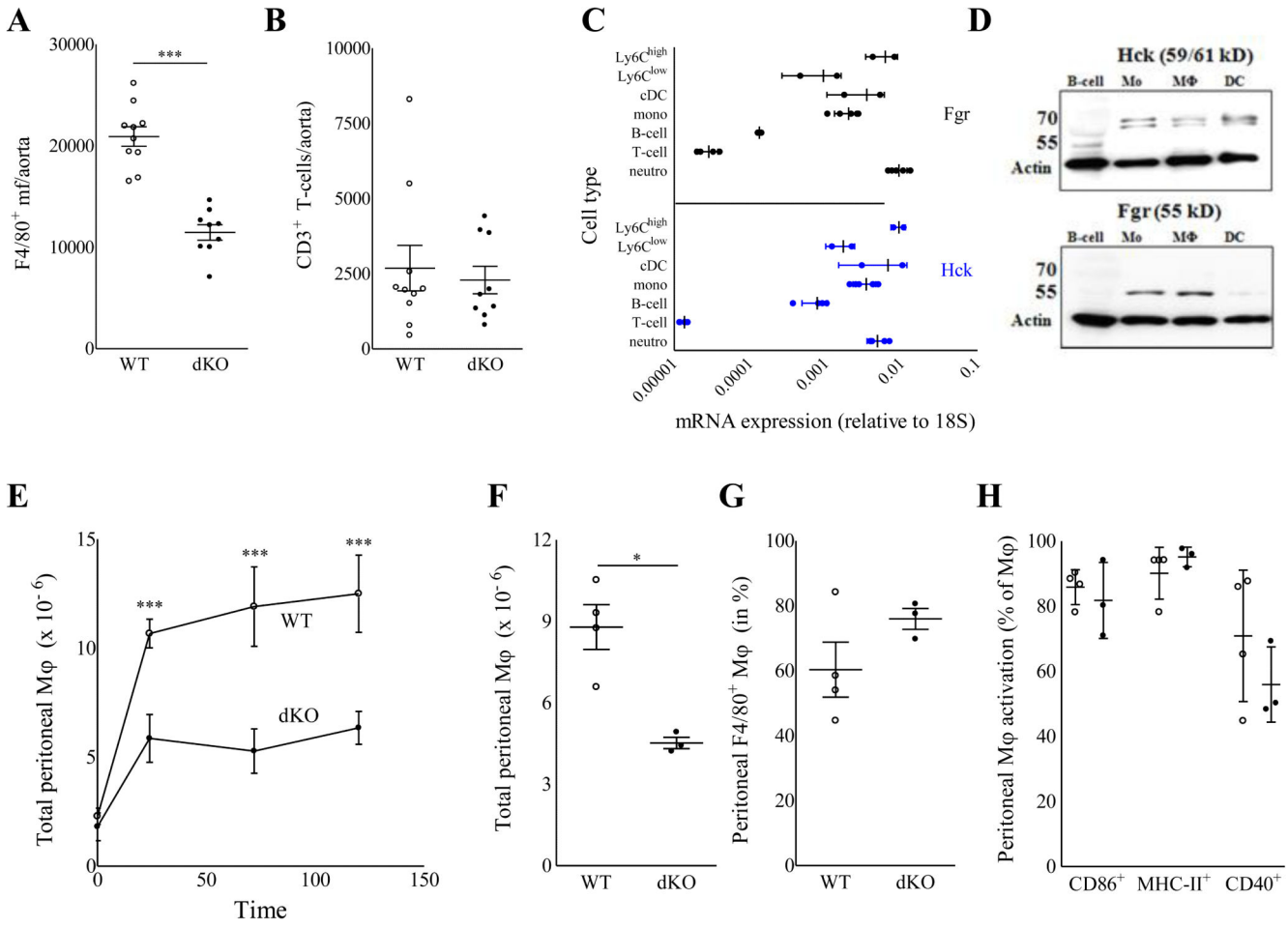

Figure 2.

A-B: Flow cytometry analysis of aorta associated leukocytes in Hck/Fgr dKO vs WT bone marrow transplanted LDLr$^{-/-}$ mice. Hck/Fgr–deficiency was associated with a reduced accumulation of F4/80^{+} macrophages (A) but had no effect on CD3+ lymphocyte contents (B) of aortas of WTD fed LDLr$^{-/-}$ mice. WT: open circles; dKO: filled circles; ***P≤0.001 (n=9). **C-D:** Expression analysis established myeloid cell specific expression of Hck and Fgr. Hck (upper panel; black symbols) and Fgr (lower panel; blue symbols) mRNA expression by monocytes (total, Ly6C^{high} and Ly6C^{low}), mDC, neutrophils B-cells and T-cells isolated by FACS from total spleen of WT and dKO chimeras; expression values are expressed relative to that of 18S (mean± S.D; n=4) (C); specific expression of Fgr and Hck by monocytes and macrophages, but not B-cells and dendritic cells (Fgr) was confirmed at protein level by Western blot analysis for Hck (59/61 kD) and Fgr (55 kD). Arrows indicate the position of 70 and 55 kD calibration markers. Beta-actin served as loading control. **E-H:** Reduced thioglycolate induced peritonitis in Hck/Fgr deficient mice. (E). The absolute levels of inflammatory cells recruited to the peritoneal cavity was reduced in dKO chimeras 24, 72 and 120 hours after intraperitoneal injection of thioglycolate. (F) Absolute monocyte/macrophage counts in peritoneal ascites were reduced by 48.5% 120 hours after induction of peritonitis in dKO chimeras. (G). Relative monocyte/macrophage numbers in the peritoneal

cavity were unchanged. (H). The expression of activation markers was not perturbed by the lack of Hck/Fgr.(n=6, duplicated samples per experimental unit). WT: open circles; dKO: filled circles; *P≤0.05, ***P≤0.001.

Europe PMC Funders Author Manuscripts

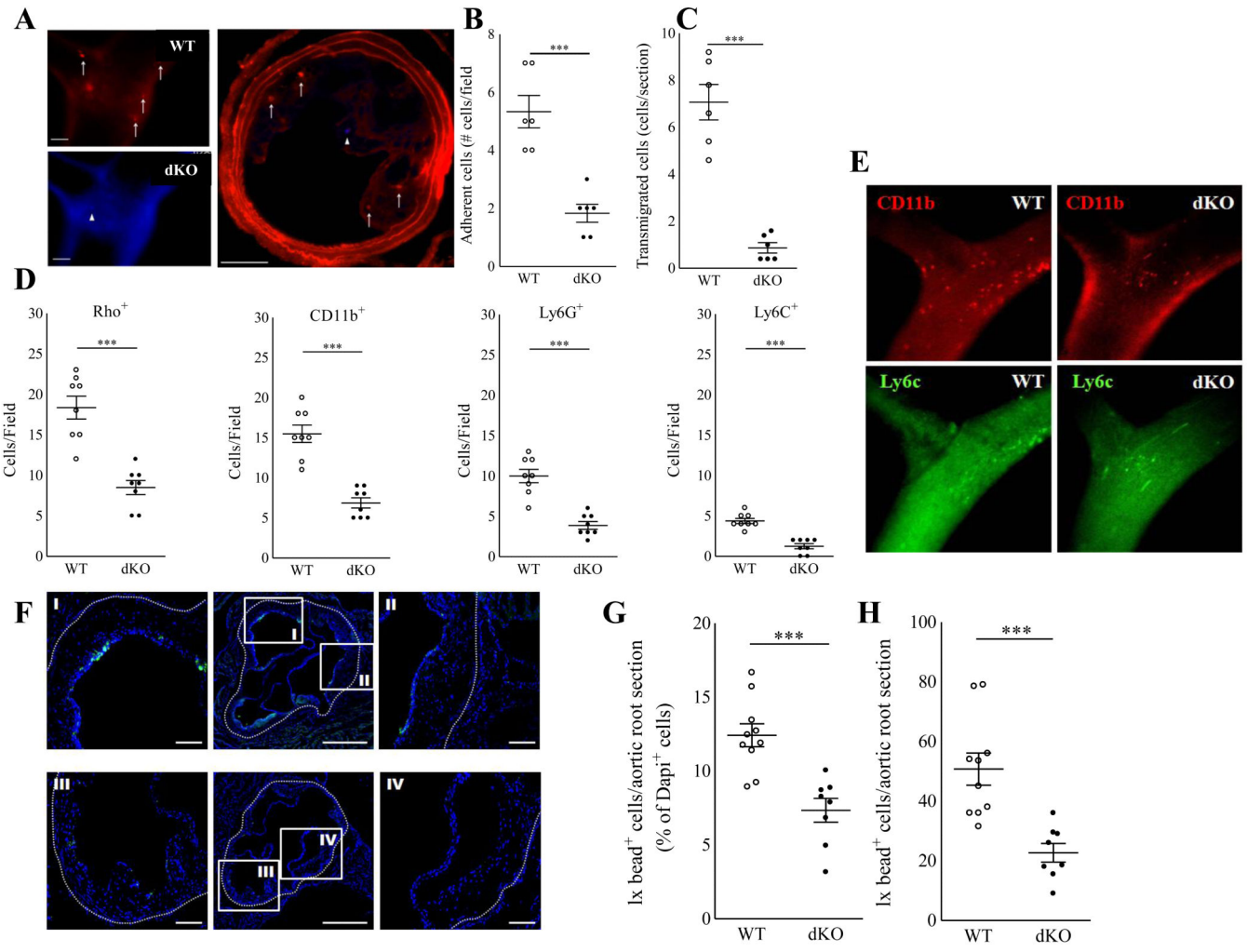

Figure 3.

Impaired adhesion to the endothelium and transmigration of Hck/Fgr-deficient macrophages in vivo. **A-C.** DAPI labeled Hck/Fgr dKO and DiI labeled WT BMDM adoptively transferred to atherosclerotic LDLr$^{-/-}$ mice ((10^6 BMDM/genotype/mouse) displayed reduced adhesion to (A+B) and transmigration (A+C) into preexisting atherosclerotic lesions induced by perivascular collar placement. Hck/Fgr dKO (arrowheads, blue) and DiI labeled WT (arrows, red) BMDM are shown to adhere and home to the central atheroma 15 min (A, left panels, intravital microscopy) and 1 day (A, right panel postmortem section) after cell co-transfer (scale bar: 100μm). D. Circulating leukocytes in atherosclerotic WT vs dKO bone marrow transplanted LDLr$^{-/-}$ with were labeled in situ with Rhodamine 6G (Rho), while in a parallel experiments monocyte subsets and neutrophils were labeled with fluorescently tagged CD11b, Ly6C and Ly6G antibodies immediately before intravital microscopy analysis at the carotid artery bifurcation (D) (n=8). DKO chimeras clearly show reduced adhesion of Rho$^+$ myeloid cells, CD11b$^+$ (all) monocytes, CD11b$^+$ Ly6C^{high} monocytes and Ly6G$^+$ neutrophils(D). (E) representative IVM pictures of monocyte adhesion in WT vs dKO chimeras (red: CD11b, green Ly6C). Circulating Ly6C^{high} monocytes were selectively labeled with fluorescent Latex Beads 72h after clodronate

liposome induced depletion of circulating monocytes in dKO and WT bone marrow transplanted $LDLR^{-/-}$ mice. Fluorescent microscopy analysis of aortic arch plaques 24h after bead injection, showed reduced presence of bead-laden macrophages in plaques of dKO chimeras (F; central panels represent overview, I and II are high power views detailing for WT mice, while III and IV are high power views of dKO mice) (n=9). Quantitative analysis of plaques confirmed significant reductions in $Ly6C^{high}$ monocyte influx, both at relative (G) and absolute (H) level. WT: open circles; dKO: filled circles; *P≤0.05, **P≤0.01, ***P≤0.001.

Europe PMC Funders Author Manuscripts

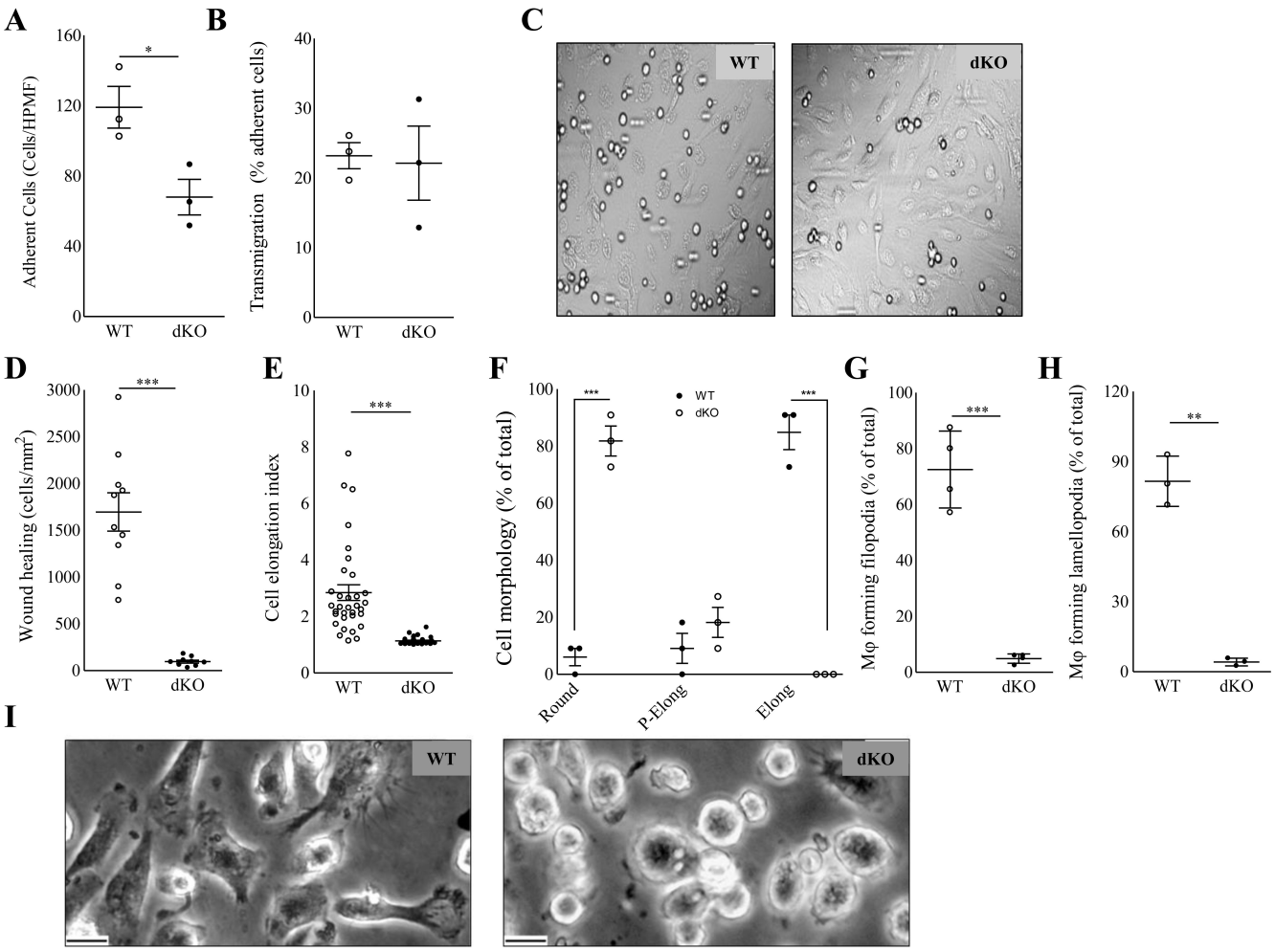

Figure 4.

Hck/Fgr dKO macrophages display impaired two dimensional directional migration and aberrant morphology. Adhesion (A) but not transmigration (B) across monolayers of inflamed endothelium *in vitro* is reduced in dKO BMDM (n=3, 6 High Power Microscopic Field (HPF) quantifications per sample). (C). Representative differential Interference Contrast microscopy HPMF pictures of BMDM adherent to inflamed endothelium *in vitro*. D. dKO macrophages display 94% reduced two dimensional migration and wound healing capacity *in vitro* (n=3, 5 area quantifications per replicate). E+F. Morphology of peritoneal macrophages (PEM) cultured for 36h (n=5, 100 cells per replicate). E. Mean elongation index (EI, defined as the ratio of cell length to cell breadth). F. Percentage of rounded (EI<1.2), partially elongated cell (1.2<EI<,2) and elongated (EI>2) and as judged by the elongation index (EI). G+H. Percentage of PEM cultured for 16 hours, forming filopodia (G) and lamellipodia (H) (n=5, 100 cells per replicate). I. Representative pictures depicting rounded cell morphology in dKO compared to WT PEM. (Scale bar: 10μm). WT: open circles; dKO: filled circles; *P≤0.05, ***P≤0.001.

Europe PMC Funders Author Manuscripts

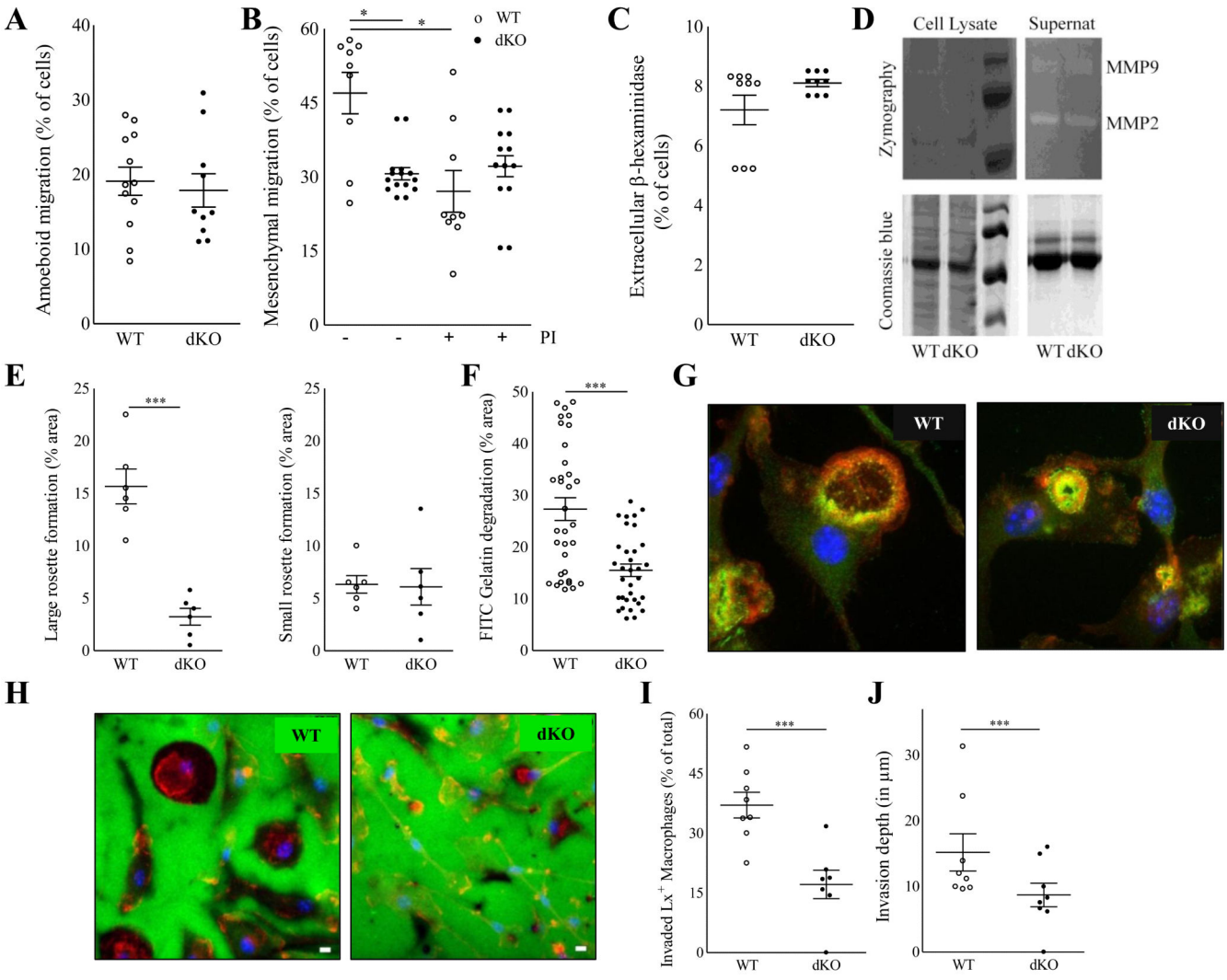

Figure 5.

Hck/Fgr deficient macrophages have impaired three-dimensional migration capacity *in vitro* and *in vivo*. Hck/Fgr-deficient BMDM displayed normal amoeboid (mean ± S.E.M. of n=12) (A) but reduced mesenchymal migration across Matrigel transwells where proteinase inhibitors (PI) inhibited WT but not dKO BMDM migration (mean ± S.E.M.; n=9-13) (B). β-hexosaminidase was released at similar levels in WT and dKO BMDM (mean ± S.D. of n=3, in triplicate) (C). Metalloproteinases MMP-2 and MMP-9 secretion, assessed by gelatin zymograph, is unaffected in dKO BMDM (D). DKO BMDM form less and smaller podosome rosettes than WT controls (n=5) (E). Representative pictures illustrating large podosome rosettes (left panel) in WT BMDM and small podosome rosettes (right panel) in dKO BMDM, 100X magnification. (F). FITC-gelatin degradation is reduced in dKO BMDM (n=3). (G+H). Representative pictures of BMDM showing fewer and smaller gelatin proteolysis areas (in dark) colocalising with podosome rosettes in dKO BMDM compared to WT controls. (Blue for cell nuclei, red for F-actin in F and H. Green for Vinculin in F, and FITC-gelatin in H). Likewise, re-inspection of the in vivo latex bead aided monocyte/macrophage tracking experiment showed that 24h after labeling the portion

of Latex bead^{+} plaque contained macrophages that had invaded into the atheroma (defined as located at > 3 μm from the endothelium) was significantly reduced in dKO chimeras (n=8) (I), while also the average plaque invasion depth of latex^{+} labeled macrophages was seen to be reduced in these mice (J). WT: open circles; dKO: filled circles; *P≤0.05, **P≤0.01, ***P≤0.001.

Europe PMC Funders Author Manuscripts

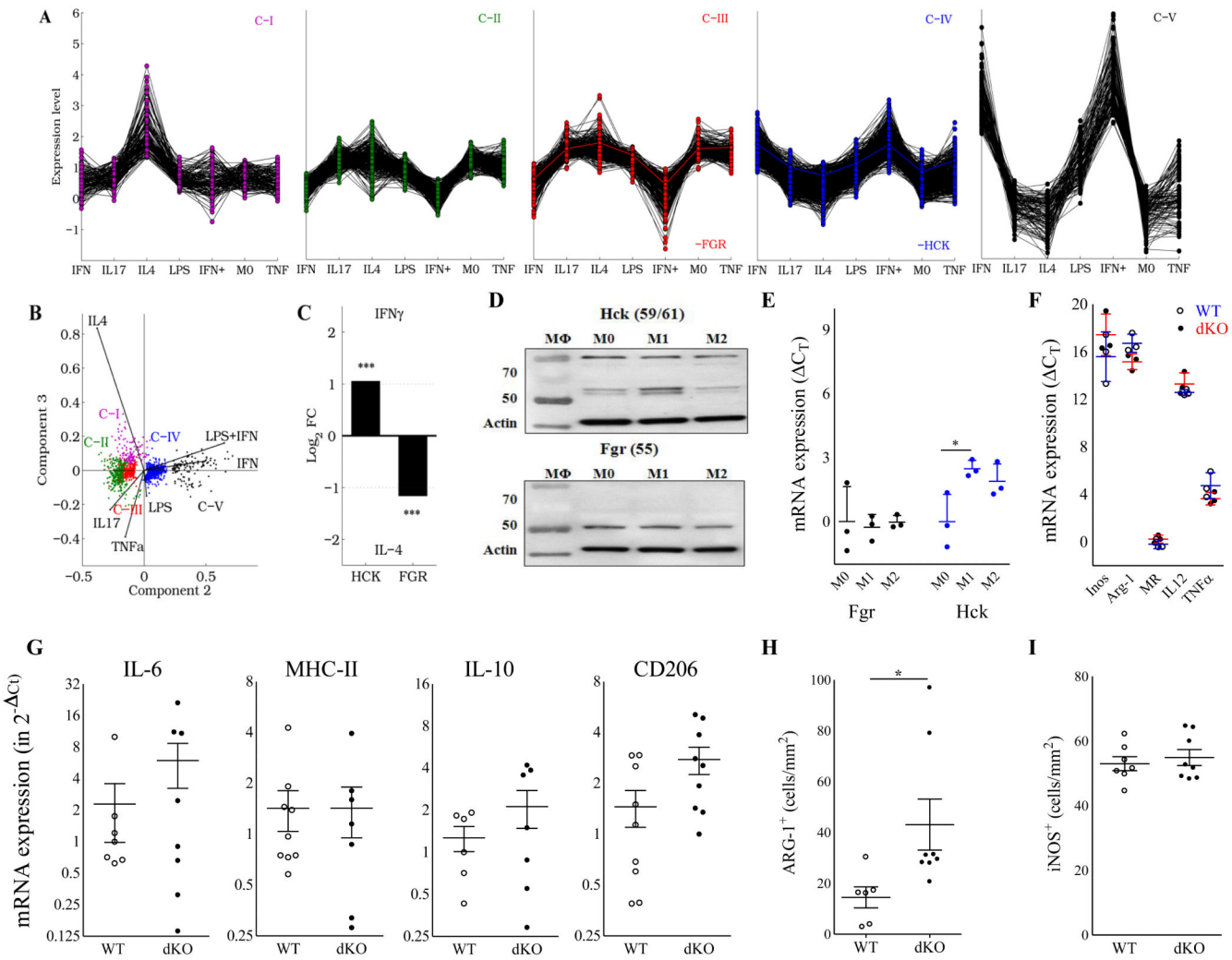

Figure 6.

Hck/Fgr are involved in separate macrophage polarization programs but their combined deficiency does not impact polarization marker expression. A. K-means clustering of human genes modulated upon stimulation with IFN-γ, IL-17, IL-4, LPS, IFN--γ +LPS (denoted as IFN^{+}) or TNF-α generates five clusters (C-I to C-V). FGR and HCK belong to C-III and C-IV, respectively, and display opposite expression patterns. B. Principal component analysis (PCA) of modulated genes. 99.3% of the variance of the system lies within the first three PC (PC1:84.8, PC2:13.2 and PC3:1.3%). C. Human HCK and FGR expression is upregulated in response to IFN-γ and IL-4, respectively. This finding was confirmed by western blotting on BMDM of WT vs dKO mice cultured in the absence (M0) or presence of IFN-γ (100U/ml, M1) or IL-4 (20ng/ml, M2) (n=3) (D). Quantification of Fgr (black symbols) and Hck (blue symbols) protein band intensities, corrected for the actin loading control (mean ± S.D.; n=3), is depicted in E. (F) mRNA expression of classical (iNOS: inducible NO synthase; IL-12; TNF-α) and alternatively activated macrophage markers (Arg-1: arginase-1 and MR: mannose receptor) in non-stimulated BMDM *in vitro* as assessed by qPCR was not affected. Relative expression was calculated using cyclophilin as housekeeping gene. QPCR data are

presented as RE+$2^{-(\Delta\Delta Ct - SD\Delta\Delta Ct)}$ and RE-$2^{-(\Delta\Delta Ct + SD\Delta\Delta Ct)}$, mean ± S.D.; n=3-4). QPCR of mRNA isolated from aorta of atherosclerotic $LDLr^{-/-}$ mice transplanted with WT and dKO bone marrow did not reveal any differences in expression of IL-6 (M1), MHC-II (M1) and IL-10 (M2), while that of CD206 (M2) was increased (G) (n=6); in agreement, immunohistochemical analysis of aorta plaques showed slightly increased arg-1 (H), but unchanged iNOS staining (I) (n=6-8). WT: open circles; dKO: filled circles.

Europe PMC Funders Author Manuscripts